anterior lens capsule. The present paper describes the characterization of the CNBr peptides of the other structurally distinct collagenous component derived from basement membrane, i.e., the D chain, which, for the present study, was prepared for kidney cortices. A similar chain was isolated in earlier studies from basement membrane structures such as anterior lens capsule, glomerular basement membrane (Dixit & Kang, 1979; Dixit, 1979), and placenta (Bailey et al., 1979; Glanville et al., 1979; Kresina & Miller, 1979; Sage et al., 1979). The CNBr peptides of the D chain described in this paper are distinct from the CNBr peptides of the C chain (Dixit & Kang, 1979), further confirming the presence of two distinct collagenous chains in basement membranes.

Acknowledgments

The authors thank Paul Jacobson and Tim Todd for their excellent technical assistance and Helen Oellerich for preparation of the manuscript.

References

Adelstein, R. S., & Kuehl, W. M. (1970) *Biochemistry 9*, 1355.
Askenasi, R. S., & Kefalides, N. A. (1972) *Anal. Biochem. 47*, 67.
Bailey, A. J., Sims, T. J., Duance, V. C., & Lights, N. D. (1979) *FEBS Lett. 99*, 361.
Bentz, H., Bachinger, H. P., Glanville, R., & Kühn, K. (1978) *Eur. J. Biochem. 92*, 563.
Brown, R. A., Shuttleworth, C. A., & Weiss, J. B. (1978) *Biochem. Biophys. Res. Commun. 80*, 866.
Burgeson, R. E., Al Adli, F. A., Kaitila, I. I., & Hollister, D. W. (1976) *Proc. Natl. Acad. Sci. U.S.A. 73*, 2579.
Chung, E., Rhodes, R. K., & Miller, E. J. (1976) *Biochem. Biophys. Res. Commun. 71*, 1167.
Crestfield, A. M., Moore, S., & Stein, W. H. (1963) *J. Biol. Chem. 238*, 622.
Crouch, E., & Bronstein, P. (1978) *Biochemistry 17*, 5499.
Daniels, J. R., & Chu, G. H. (1975) *J. Biol. Chem. 250*, 3531.
Dehm, P., & Kefalides, N. A. (1978) *J. Biol. Chem. 253*, 6680.
Dixit, S. N. (1978) *FEBS Lett. 85*, 153.
Dixit, S, N. (1979) *FEBS Lett. 106*, 379.
Dixit, S. N., & Kang, A. H. (1979) *Biochemistry 18*, 5686.
Duance, V. C., Restall, D. J., Beard, H., Bourne, F. J., & Bailey, A. J. (1977) *FEBS Lett. 79*, 248.
Freytag, J. W., Ohno, M., & Hudson, B. G. (1976) *Biochem. Biophys. Res. Commun. 72*, 796.
Glanville, R. W., Rauter, A., & Fietzek, P. P. (1979) *Eur. J. Biochem. 95*, 383.
Heathcote, J. G., Sear, C. H. J., & Grant, M. E. (1978) *Biochem. J. 176*, 283.
Hudson, B. G., & Spiro, R. G. (1972) *J. Biol. Chem. 247*, 4229.
Kang, A. H. (1972) *Biochemistry 11*, 1828.
Kefalides, N. A. (1971) *Biochem. Biophys. Res. Commun. 45*, 226.
Kefalides, N. A. (1972) *Biochem. Biophys. Res. Commun. 47*, 1151.
Kresina, T. F., & Miller, E. J. (1979) *Biochemistry 18*, 3089.
Laemmli, U. (1970) *Nature (London) 227*, 680.
Miller, E. J. (1972) *Biochemistry 11*, 4903.
Minor, R. R., Clark, C. C., Strause, E. L., Koszalka, T. R., Brent, R. L., & Kefalides, N. A. (1976) *J. Biol. Chem. 251*, 1789.
Piez, K. A. (1968) *Anal. Biochem. 26*, 305.
Piez, K. A., Weiss, E., & Lewis, M. S. (1960) *J. Biol. Chem. 235*, 1978.
Rhodes, R. K., & Miller, E. J. (1978) *Biochemistry 17*, 3442.
Sage, H., & Bornstein, P. (1979) *Biochemistry 18*, 3815.
Sage, H., Woodbury, R. G., & Bornstein, P. (1979) *J. Biol. Chem. 254*, 9893.
Sato, T., & Spiro, R. G. (1976) *J. Biol. Chem. 251*, 4062.
Schwartz, D., & Veis, A. (1978) *FEBS Lett. 85*, 326.
Timpl, R., Martin, G. R., Bruckner, P., Wick, G., & Wiedmann, H. (1978) *Eur. J. Biochem. 84*, 43.
Trelstad, R. L., & Lawley, K. R. (1977) *Biochem. Biophys. Res. Commun. 76*, 376.
von der Mark, H., & von der Mark, K. (1979) *FEBS Lett. 99*, 101.

Turbidity Measurements in an Analytical Ultracentrifuge. Determinations of Mass per Length for Filamentous Viruses fd, Xf, and Pf3†

S. A. Berkowitz‡ and L. A. Day*

ABSTRACT: An analytical ultracentrifuge has been used to measure light-scattering intensities by the transmittance method. The technique, which is applicable to particles of many sizes and shapes, has the principal advantage that samples can be kept free of dust during the measurements. Also, sample volumes are small, and the scanner and interference optics can be used simultaneously to obtain, for a given sedimenting boundary, turbidity steps at different wavelengths and the concentration step. In the present application the data yield mass per length estimates for three filamentous viruses, 19 100 daltons/nm for fd, 19 600 daltons/nm for Pf3, and 19 100 daltons/nm for Xf.

Measurements of the turbidity, τ, as a function of wavelength provide the same type of information on molecular weights and dimensions of macromolecules in solution as measurements of the angular dependence of the Rayleigh ratio (Heller & Vassy, 1946; Heller et al., 1946; Cashin & Debye, 1949; Doty & Steiner, 1950). Recent papers have dealt with applications to a variety of biological systems [e.g., Camerini-Otero et al. (1974), Gaskin et al. (1974), and Carr & Hermans (1978)] and with methods for interpreting data gathered as a function of wavelength (Camerini-Otero & Day,

† From The Public Health Research Institute of The City of New York, New York, New York 10016. *Received August 22, 1979.* This work was supported by Grant AI 09049 from the U.S. Public Health Service.

‡ Present address: National Institute of Arthritis, Metabolism and Digestive Diseases, National Institutes of Health, Bethesda, MD 20205.

0006-2960/80/0419-2696$01.00/0

1978). In the case of scatterers that are long rods, the particle scattering functions can be integrated over all scattering directions to obtain mass per length from turbidity data (Berne, 1974; Carr & Hermans, 1978). In this study we have obtained a value for the mass per length of fd virus in reasonable agreement with recent literature values by other techniques. Account has been made for small effects of anisotropy according to functions derived by Horn et al. (1951). We have also collected turbidity data for Xf, a virus of *Xanthomonas orzyae* (Kuo et al., 1967) that is 1.0 μm long, and for Pf3, a virus which infects *Pseudomonas aeruginosa* bearing the RP1 plasmid (Stanisich, 1974) and which is about 0.7 μm long, and have obtained mass per length values in solution for these viruses. A preliminary account of some of this work has been published (Berkowitz & Day, 1979).

The instrument used for turbidity measurements, as well as for refractive index increment and concentration measurements, was an analytical ultracentrifuge equipped with an absorption optical system and an interference optical system. Earlier measurements on R17, a small icosahedral virus, showed to us the convenience and simplicity of using the analytical ultracentrifuge for turbidity measurements (Berkowitz, 1975). Its use allows one to obtain easily samples that are free of dust and spurious aggregates, thus solving the persistent problem of sample clarification for light-scattering measurements [see, for example, discussions by Timasheff & Townsend (1970), Eisenberg (1971), Tabor (1972), and Godfrey & Eisenberg (1976)]. Its use also satisfies the need for a detection system that views only a small solid angle in the forward scattering direction (Gumprecht & Sliepcevich, 1953; Heller & Tabibian, 1957).

Experimental Procedures

Virus Samples. fd was grown on *Escherichia coli* 3300, concentrated by poly(ethylene glycol) precipitation (Yamamoto et al., 1970), and then purified by resuspension and a second polymer precipitation, followed by differential sedimentation and equilibrium banding in a CsCl gradient. The infectivity of the preparation used was 0.3 plaque former/physical particle, somewhat lower than usual. The autocorrelation functions determined on aliquots of this preparation (Newman & Carlson, 1980) gave the diffusion coefficient obtained previously on samples known to be nearly monodisperse with respect to length (Newman et al., 1977). Concentrations were determined with an extinction coefficient of 3.84 mg^{-1} cm^2 at 269 nm (Berkowitz & Day, 1976); the OD_{269}/OD_{244} ratio was 1.41.

Two Pf3 bacteriophage preparations were made from single plaque isolates from a lysate provided by Dr. D. E. Bradley. The host, *P. aeruginosa PAO* 8 (RP1), was also provided by Dr. Bradley. It was found (G. Switz, L. Day, and R. L. Wiseman, unpublished experiments) that Pf3 could be conveniently grown to raw titers of 2×10^{11} plaque formers/mL and concentrated from the medium with poly(ethylene glycol) as can other filamentous viruses but that Pf3 precipitates at its buoyant density of ~1.29 in CsCl. The preparation of one Pf3 sample included CsCl density banding, but the preparation of a second sample consisted merely of two precipitations from 0.5 M NaCl and 2% poly(ethylene glycol). The infectivity of both Pf3 preparations was about 0.2 plaque former/physical particle. Samples of Xf virus were provided to us by Dr. R. L. Wiseman.

Pf3 viral DNA was prepared by three extractions with buffer-saturated phenol at ~60 °C. The phenol was removed from the aqueous phases with ether, which was subsequently removed by aeration and dialysis. ϕX174 DNA was kindly made available to us by Dr. F. Sanger.

Instrumentation. The analytical ultracentrifuge used as the light-scattering instrument was a Beckman Model E equipped with a conventional photoelectric scanner system and a Rayleigh interference optical system. The source lamp for the scanner was a medium-pressure xenon lamp containing mercury. The Hg spectral lines used for τ measurements were those at 365.5, 405.0, 435.8, and 546.1 nm. Lines at 266, 313, and 334 nm were used for concentration measurements. The lines were located by adjusting the monochromator to minimum dynode voltage (maximum light intensity) in the region of the desired line. The ultracentrifuge cells used were either the six-channel external loading cells of the Yphantis type (these cells do not have sector shapes) or the conventional two-channel, 2.5° sector-shaped cells. Cells having 12- and 30-mm path lengths were used. Capillary-type boundary-forming cells were used for some of the refractive index measurements. The windows were quartz, and window holders masked the cells with either 0.5- or 2.4-mm apertures. The overall configuration of the scanner optics can be described briefly as follows, starting at the monochromator exit as position 0 cm along the "optical bench". The vertical divergent beam is collected by a cylindrical lens of focal length (f) = 10 cm at 20 cm. The beam then passes through a collimating lens (f = 89 cm) at 83 cm. The optical cell assembly is centered at ~95 cm. The condensing lens (f = 74 cm) with a mask of 5-mm slit width is at 107 cm. Two front surface mirrors at 160 and 166 cm (combined f = 40 cm) deflect the beam horizontally and focus an image of the cell sector, magnified by a factor of 2, on the photomultiplier entrance slit, usually set at 0.22 mm, located at 269 cm at the end of the optical bench. Our calculations of solid angles viewed by the detector give an angle of less than 0.6° as an average over the entire sample volume and a maximum angle of 0.9° for the volume element closest to the detector. The effects of the solid angles on the final result depend on the shape and size of the scatterer (Gumprecht & Sliepcevich, 1953; Heller & Tabibian, 1957). We used solutions of methyl red dye at neutral pH to confirm the photometric accuracy of the scanner optics and electronics through comparisons with absorbance measurements in Cary 14 and Zeiss PMQII spectrophotometers. The absorbance spectrum of this dye has broad maxima and minima centered at or near the wavelengths of the mercury emission lines of the source lamp, thus making it a convenient standard.

The measurements of τ, in ideal cases, are done by first sedimenting the boundary of a component of interest to a position where it is resolved from other boundaries. Then, at the same or a much slower centrifuge speed, scans of turbidity steps across the boundary at several wavelengths are made. Photographs of the fringe pattern of the refractive index gradient can be made with the interference optics system to obtain concentrations, simultaneously with the scans. Centrifugation is then continued until reference base line turbidity scans and refractive index gradient photographs appropriate for the given boundary can be taken. The turbidity steps and the exact concentration step between any two exactly known radial positions on either side of a given boundary can then be obtained from the two sets of data.

dn/dc Measurements. Method 1. fd virus solutions of 1.5 mL were dialyzed at room temperature against 0.15 M KCl and 1 mM sodium phosphate buffer, pH 7. Buffer solutions of 1.5 mL were also placed in dialysis bags and equilibrated against the same outer buffer solutions. The dialysis system was in a sealed 500-mL container rotated at 0.2 rpm for ~24

h; the inner and outer solutions were gently mixed by the movement of air bubbles. The sample and buffer blank solutions, handled identically, were transferred to the appropriate sectors of a capillary-type, double-sector boundary-forming cell of 12-mm path length that had been assembled with interference masks. The cell was accelerated to 6000 rpm in an AN-D rotor. Interference patterns generated by the newly formed boundary were photographed less than 4 min after reaching speed so that sedimentation of the boundary was negligible. The rotor was stopped, shaken, and accelerated again, and base line reference patterns were photographed. The wavelength for interference work was 546.1 nm. Total fringes were determined with a Gaertner microcomparator. The concentrations were obtained from measurements of optical densities at 269 nm in a Cary 14 spectrophotometer. The number of fringes, the concentration, the optical path, and the wavelength of light were used to calculate the specific refractive index difference, $\Delta n/\Delta c$.

Method 2. The samples of fd virus in the same buffer as in method 1 were placed in six-channel side-access cells (Ansevin et al., 1970) assembled with interference masks. Interference patterns were photographed at various times during sedimentation and after the material had sedimented to the bottom. The number of fringes and the radial position of the sedimenting boundaries were established in one or more photographs. The number of hypothetical fringes prior to sedimentation was obtained by calculations on the basis of assumed dilutions depending on the square of the radius, even though this was a slight underestimate because of the nonsector shape of the six-channel cell and the position of the interference masks. The concentrations of the samples were obtained as described in method 1.

Method 3. Samples of fd virus were placed in double-sector cells assembled with interference masks. Photographs of the interference patterns and scans of the boundaries at 266 nm were made simultaneously while the boundaries sedimented. The absorbance difference between two radial points on either side of the boundary and the refractive index difference between these same two points were used to obtain $\Delta n/\Delta c$ for the virus in the freely sedimenting boundary.

Ancillary Techniques. Size of Pf3 Viral DNA. The sedimentation velocity of Pf3 DNA relative to ϕX174 DNA in alkaline conditions was determined by running three samples of each viral DNA in band-forming cells in an AN-F rotor in each of two runs. Time points for peaks for the circular forms in each DNA sample were recorded to obtain a sedimentation velocity ratio of 1.042 ± 0.011 for Pf3 DNA relative to ϕX174 DNA. The exact number of nucleotides in both ϕX174 DNA, 5386 (Sanger et al., 1978), and fd DNA, 6408 (Beck et al., 1978), and their relative sedimentation velocity of 1.072 in 0.9 M NaCl and 0.1 M NaOH (Day & Berkowitz, 1977) give a value of 0.400 for the exponent in $(6408/5386)^a = 1.072$. This is the same exponent found by Studier (1965), and it gives $(5386)(1.042 \pm 0.011)^{2.5} = 5960 \pm 180$ for the number of nucleotides in Pf3 DNA.

Electron Microscopy. Mixed and separate solutions of 2 μg/mL fd virus and 2 μg/mL Pf3 virus in ~0.1 mM KCl were prepared by diluting virus stock solutions with distilled water. Droplets of 5 μL were placed on carbon grids. After 30 s the drop was removed by filter paper. The grids were then shadow cast with platinum from two directions at approximately right angles to each other at a shadow angle of ~10°. Fields which contained about 15–30 particles were photographed at a nominal magnification of 7000 with a Phillips 300 electron microscope in the bright field mode. The relative lengths of enlarged images of the fd and Pf3 particles (images of approximately 3.2 and 2.5 cm, respectively) were obtained with the aid of a Numonics digital planimeter with a repeatability of ±0.03 cm/measurement. The average length of Pf3 relative to fd was determined to be 0.774 ± 0.003. Taking the absolute electron microscopic (EM) length of fd to be 0.882 ± 0.008 μm (Frank & Day, 1970; Wall, 1971; see Day & Wiseman, 1978), we obtain 0.683 ± 0.008 as the EM length of Pf3. The length of Pf3 of 0.76 μm reported by Bradley (1974) differs from the value we have obtained. We do not know the reason for this, but the difference of ~11% leads to an uncertainty of only 1% in the final calculated mass per length of Pf3, as explained below.

Turbidity Equations. The turbidity equation for light scattering by large macromolecules of any shape at infinite dilution is

$$\tau(\lambda_0) = H(\lambda_0)cM_rQ(\lambda_0) \quad (1)$$

where λ_0 is the wavelength in vacuo, $\tau(\lambda_0)$ is 2.303 × the optical density per centimeter of light path through the solution, c is the concentration in g cm^{-3}, M_r is the molecular weight, and $H(\lambda_0)$ is the constant given by

$$H(\lambda_0) = (32\pi^3/3N_A)n_0^2(\partial n/\partial c)_\mu^2\lambda_0^{-4} \quad (2)$$

in which N_A is Avogadro's number, n_0 is the refractive index of the solvent, $(\partial n/\partial c)_\mu$ is the refractive index increment of the scatterer at infinite dilution and in chemical equilibrium with all components of the system (Casassa & Eisenberg, 1964), and $Q(\lambda_0)$ is the transmittance equivalent of the particle-scattering factor $P(\theta)$ given by

$$Q(\lambda_0) = (3/8)\int_0^\pi [P(\theta)(1 + \cos^2\theta)](\sin\theta)\, d\theta \quad (3)$$

Values of $Q(\lambda_0)$ have been calculated for isotropic rods, spheres, and random coils (Doty & Steiner, 1950; Camerini-Otero & Day, 1978). For anisotropic rods of length L and anisotropy δ, $Q(\lambda_0)$ becomes

$$Q(\lambda_0) = (3/8)\int_0^\pi [V_v(x,\delta) + 2H_v(x,\delta) + H_h(x,\delta)](\sin\theta)\, d\theta \quad (4)$$

where the total intraparticle interference is given by the sum of three terms that are functions of $x = (2\pi Ln_0/\lambda_0)\sin(\theta/2)$ and the anisotropy, $\delta = (\alpha - \beta)/(\alpha + 2\beta)$, where α and β are the polarizabilities parallel and perpendicular to the axis, respectively. The terms V_v, H_v, and H_h account for interference effects in horizontally and vertically polarized components of the scattered light (Horn et al., 1951; Horn, 1955). For $\delta = 0$, eq 4 reduces to eq 3 with $P(\theta) = \mathrm{Si}(2x)/x - \sin^2 x/x^2$, the classical scattering function for isotropic rods. We have found the complete expressions for V_v, H_v, and H_h for rods of any L and δ to be unsuitable for simple numerical evaluation of $Q(\lambda_0)$ according to eq 4, so exact corrections of turbidity data for short and moderate length anisotropic rods are not presently available. However, the approximate expressions for V_v, H_v, and H_h given by Horn et al. (1951) for rods of "infinite" length do allow the integration of eq 4, yielding

$$Q(\lambda_0)_{\text{infinite rods}} = (11/20)(\lambda_0/n_0L)(1 + 2\delta/11 + 23\delta^2/11) \quad (5)$$

Equations 1 and 5 give the expression

$$\tau(\lambda_0) = (88\pi^3/15N_A)[n_0(\partial n/\partial c)_\mu^2/\lambda_0^3] \times (1 + 2\delta/11 + 23\delta^2/11)(M_r/L)c \quad (6)$$

Table I: Estimates of Mass per Length of fd, Pf3, and Xf from Turbidity Data[a]

	fd virus			Pf3 virus			Xf virus		
λ_0	τ/c (g^{-1} cm^2)	Q	M_r/L (daltons/nm)	τ/c (g^{-1} cm^2)	Q	M_r/L (daltons/nm)	τ/c (g^{-1} cm^2)	Q	M_r/L (daltons/nm)
365.5	53.5	0.144	19 400	57.0	0.192	20 800	56.0	0.139	19 700
405.0	37.0	0.165	19 600	35.6	0.211	19 000	38.5	0.153	19 700
435.8	26.9	0.177	18 600	28.7	0.225	20 000	28.0	0.163	18 700
546.1	13.2	0.217	20 100						
av:			19 400 ± 600			19 900 ± 900			19 400 ± 600
cor for anisotropy:			19 100 ± 600			19 600 ± 900			19 100 ± 600

[a] The uncertainties are standard deviations which, together with possible systematic errors, give overall uncertainties of ~10% (see text). Values of Q were calculated from eq 3 with the following values for L: 0.895 μm for fd (Newman et al., 1977), 0.68 μm for Pf3 (this study), and 0.98 μm for Xf (Kuo et al., 1967; Chen et al., 1980).

This relationship for the case $\delta = 0$ was obtained by Berne (1974) and Carr & Hermans (1978). It is seen that M_r/L for an infinite rod is given directly by absolute measurements of turbidity; our calculations show that for $n_0L/\lambda_0 > 30$ and $\delta = 0$, values of M_r/L from eq 6 are within 2% of the true values. However, the ratios n_0L/λ_0 encountered in this study fall between 1.7 and 4.2 so that eq 3 was used to calculate Q values with the initial assumption that $\delta = 0$. A correction factor of 1.016 for anisotropy was then introduced. It was calculated from the anisotropy term in eq 6 with $\delta = 0.054$ obtained for fd at 546 nm (Berkowitz & Day, 1976); the same factor was used for the three viruses at the various wavelengths. The viruses are so long that residual uncertainties in L of 10% or less lead to uncertainties in M_r/L of less than 1%. Also, the large L makes the small anisotropy correction a good first approximation, but the overall uncertainty from this source could be as high as 4% in M_r/L.

The values of $(\partial n/\partial c)_\mu$ and n_0 were obtained from $(\partial n/\partial c)_\mu = (\partial n(546)/\partial c)_\mu(0.925 + 2.2 \times 10^4\ nm^2/\lambda_0^2)$ and $n_0(\lambda_0) = n_0(546)(0.992 + 2.31 \times 10^3\ nm^2/\lambda_0^2)$ from Camerini-Otero & Day (1978).

Results

Refractive Index Increments. Values of $\Delta n/\Delta c$ obtained for fd at 546 nm are plotted in Figure 1 as a function of concentration. There is no apparent systematic difference between the three methods used and no apparent concentration dependence. Accordingly, the average value from all eight measurements, 0.178 ± 0.005 g^{-1} cm^3, was taken as the value of $(\partial n/\partial c)_\mu$. It is substantially lower than our earlier value of 0.191 g^{-1} cm^3 for fd (Berkowitz & Day, 1976), which was apparently erroneous because of systematic errors at low concentrations that led to an artifactual concentration dependence. Measurements of $\Delta n/\Delta c$ for Pf3 and Xf have not been carried out; the value 0.180 g^{-1} cm^3 for $(\partial n/\partial c)_\mu$ at 546 nm was assumed for each of these viruses.

The values of $(\partial n/\partial c)_\mu$ and of M_r in eq 1 pertain to the species for which concentrations are determined, namely, in the case of fd, the presumably dry material weighed out for the extinction coefficient determinations (Berkowitz & Day, 1976). The correct value of M_r (and M_r/L) for this material is given by eq 1 if $(\partial n/\partial c)_\mu$ is measured under conditions of thermodynamic equilibrium of diffusible components (Casassa & Eisenberg, 1964). In method 1 for $(\partial n/\partial c)_\mu$ we assume thermodynamic equilibrium was attained during dialyses. For methods 2 and 3, the macromolecular species were freely and slowly sedimenting in the buffer solution during the measurements, so that the values of $\Delta n/\Delta c$ obtained by these methods are unambiguously the values for thermodynamic equilibrium. For this reason and because one can avoid possible artifacts on sample handling in a dialysis experiment, we feel that methods 2 and 3 are preferable.

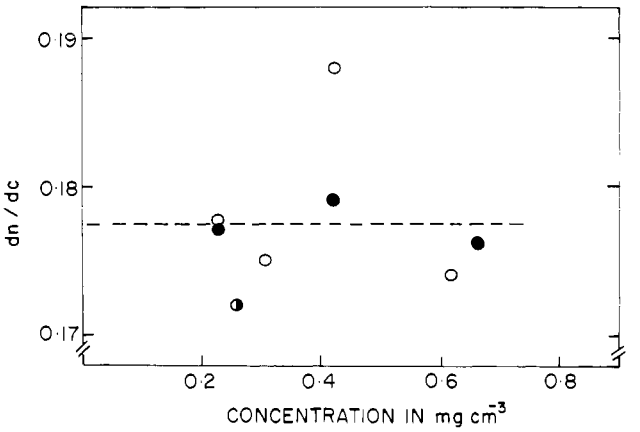

FIGURE 1: Refractive index increments for fd virus in 0.15 M KCl and 1 mM sodium phosphate, pH 7.0, obtained with the analytical ultracentrifuge according to methods 1 (○), 2 (●), and 3 (◑) described in the text.

Mass per Length. fd virus has been well characterized with respect to length (Frank & Day, 1970; Wall, 1971; Newman et al., 1977) and to mass (Newman et al., 1977), especially since the number of nucleotides in its DNA has been determined (Beck et al., 1978) and the DNA content in the virion is known (Marvin & Hohn, 1969; Berkowitz & Day, 1976). If one accepts 895 nm as the length of fd virus in solution and 16.4×10^6 daltons as its mass (Newman et al., 1977), then its mass per length is 18 300 daltons/nm.

The turbidity data for fd are extrapolated to zero concentration in Figure 2, and the intercept values of τ/c were used to obtain M_r/L according to eq 1 and 3. The actual measured absorbancies ranged from ~0.016 at the lowest concentration and longest wavelength to ~0.16 at the highest concentration and shortest wavelength. The results are listed in Table I. The estimate of M_r/L of 19 100 daltons/nm for fd virus, given by the turbidity method developed here, is in satisfactory agreement with the expected value. This supports the reliability and utility of the method. An additional value of 18 000 daltons/nm is obtained from our earlier light-scattering data at high angles (Berkowitz & Day, 1976) if the new value of 0.178 g^{-1} cm^3 is used for $(\partial n/\partial c)_\mu$.

Samples of Pf3 and Xf viruses contained aggregated material, but hypersharp sedimentation boundaries characteristic of highly purified filamentous viruses could be obtained after several minutes of sedimentation at speeds between 20 000 and 30 000 rpm. Experiments were done in two stages to ascertain the concentration steps across the boundaries. First, absorbance steps at 313 or 334 nm were related to concentration steps by means of simultaneous scanner traces and interference photographs under suitable experimental conditions. Then,

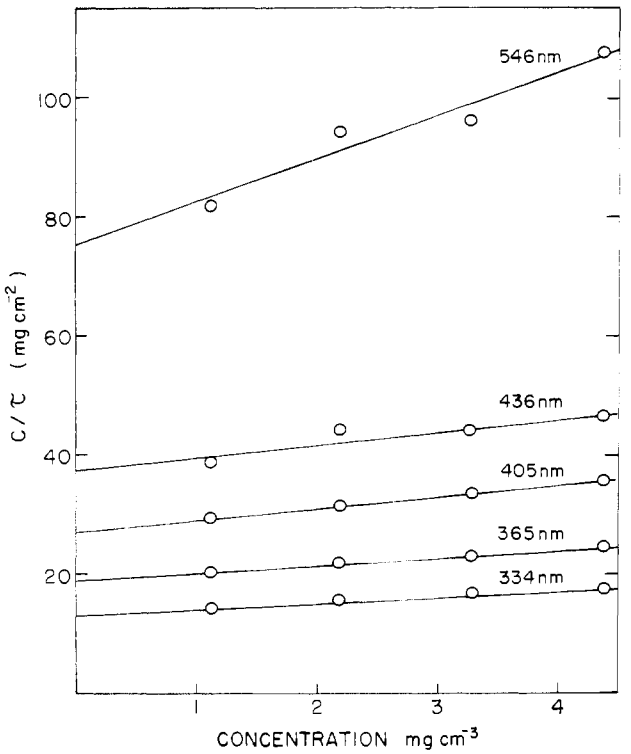

FIGURE 2: Reciprocal plot of turbidity results for fd virus in 0.15 M KCl and 1 mM sodium phosphate, pH 7.0, obtained from measurements in the analytical ultracentrifuge. The positive slopes are consistent with expected virial effects for nonaggregating systems. The intercept values at $c = 0$ were used for calculations of M_τ/L (Table I).

in 30-mm path cells assembled without the interference masks for turbidity measurements at 366, 405, and 436 nm, concentrations were obtained from optical density measurements at 313 or 334 nm.

The turbidity data for Pf3 are shown in Figure 3, and those for Xf are shown in Figure 4. In both cases, the concentration dependence of c/τ has a zero or slightly negative slope, rather than the positive slope observed for fd. This is consistent with an apparent stronger tendency toward aggregation. The values of M_τ/L calculated from the intercepts at zero concentration are listed in Table I with the results for fd.

Systematic uncertainties in such measurements are from three principal sources: concentrations, anisotropies, and lengths. The combined uncertainties in concentration and $(\partial n/\partial c)_\mu$ are estimated at 3% for fd but at 5% for Pf3 and Xf. When concentrations of solutions used for light scattering are obtained from Δn measurements, the uncertainty in the value of $(\partial n/\partial c)_\mu$ enters eq 1 in an inverse-linear way rather than in an inverse-quadratic way. This can be seen by substitution of $c = \Delta n/(\partial n/\partial c)_\mu$ in eq 1. Thus, if a $(\partial n/\partial c)_\mu$ value, either measured or assumed, were 3% too low, then M_τ/L would be 3% too high. The uncertainties from L and δ were discussed above and lead to less than 5% error in M_τ/L. In summary, considerations of possible systematic errors combined with the random uncertainties given by the data lead us to an estimate of overall uncertainty of no more than 10% in the corrected average M_τ/L values given in Table I for the three filamentous viruses.

Discussion

Turbidity measurements in the analytical ultracentrifuge were used by Josephs & Harrington (1967) to detect changes in myosin aggregation with pressure and, more recently, by

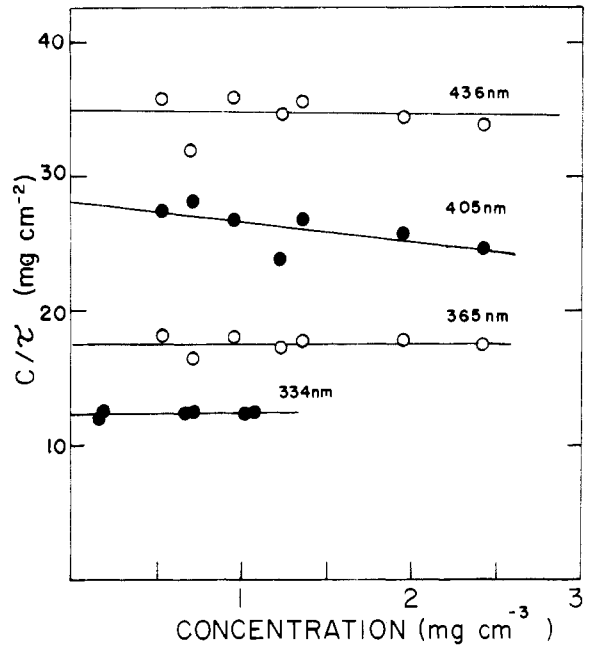

FIGURE 3: Reciprocal plot of turbidity results for Pf3 virus in 0.15 M NaCl and 0.015 M sodium phosphate, pH 7, obtained from measurements in the analytical ultracentrifuge. The apparent negative slopes may reflect the tendency of Pf3 to aggregate in the preparations used. The intercept values at $c = 0$ from least-squares analyses of the data at 365.5, 405, and 435.8 nm were used for calculations of M_τ/L (Table I). The turbidity data at 334 nm were used to establish concentrations, as described in the text.

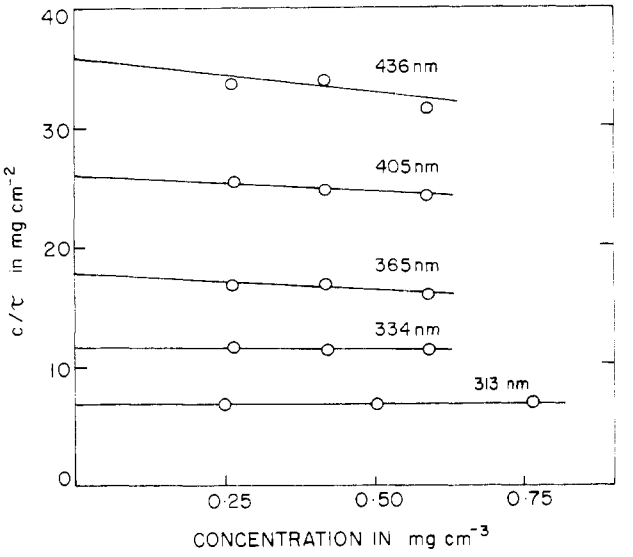

FIGURE 4: Reciprocal plot of turbidity results for Xf virus in 0.15 M NaCl and 0.015 M sodium phosphate, pH 7, obtained from measurements in the analytical ultracentrifuge. The apparent negative slopes may reflect the tendency of Xf to aggregate in the preparations used. The intercept values at $c = 0$ from least-squares analyses of the data at 365.5, 405, and 435.8 nm were used for calculations of M_τ/L (Table I). The turbidity data at 313 nm were used to establish concentrations, as described in the text. The concentrations for measurements at 313 nm were twice those given by the abscissa scale.

Ma et al. (1977) to detect aggregates of low-density lipoproteins in a study of size heterogeneity by sedimentation velocity. In the present study, which follows earlier work by Berkowitz (1975), we have used the analytical ultracentrifuge as the light-scattering instrument itself and have gathered turbidity data as a function of wavelength for use in the classical light-scattering equations. In so doing we have recognized some advantages it has over conventional light-

scattering instruments. Measurements can be made on small sample volumes, on the order of 100 μL, which can be kept free of dust by the centrifugal field during the measurements. The availability of high-intensity emission lines from the mercury in the source lamp gives good instrument performance and accurate wavelengths. Although not used in this study, this allows the dimensions of some scatterers to be accurately determined (Doty & Steiner, 1950; Camerini-Otero & Day, 1978). The analytical centrifuge can also be used to measure the critical parameter $(\partial n/\partial c)_\mu^0$ and, through it, the concentration (Babul & Stellwagen, 1969). As shown in this study, the interference and scanner optical systems can be used simultaneously to obtain values of τ/c for a given boundary in a sedimentation experiment. Hence, the essential parameters required for the turbidity method can be determined under controlled conditions with this one instrument. This allows, in principle, the characterization of an individual component of a solution of macromolecules by its sedimentation coefficient, its radius of gyration, its virial coefficient, and its molecular weight. In addition, point by point measurements across a concentration gradient in a single centrifuge cell might give the mass, the size, and the thermodynamic virial coefficients for a homogeneous scatterer or might give useful information about the mode of aggregation in interacting systems. Considerable information about a number of variables affecting the light scattering by a given macromolecular system, such as pressure or sample heterogeneity, could be obtained by this method.

It was our interest in the structure of filamentous viruses and the need for mass per length values that led to this development of the ultracentrifuge method. It has already been noted by Newman et al. (1977) that the mass per length of fd virus converts to almost exactly 10 subunits and 23 ± 1 nucleotides in the approximate structure repeat of 3.2 nm given by the X-ray patterns (Marvin et al., 1974b), and this has been used as a guide in an interpretation of the X-ray patterns (Makowski & Caspar, 1978). The value of 19 100 daltons/nm (±10%) for Xf in solution converts to 29 ± 3 protein subunits/7.7-nm repeat observed for wet fibers by X-ray diffraction (Marvin et al. 1974a), if one assumes 87% protein (Wiseman & Day, 1977) and a subunit molecular weight of 4343 (Frangione et al., 1978). This agrees with an estimate of 28 ± 2 subunits/structure repeat on the basis of DNA molecular weight, chemical composition, and virus length (Wiseman & Day, 1977; Day & Wiseman, 1978). The M_r/L value for Pf3 obtained here is the only one available. Combining it with the DNA size and the length obtained in this study, we estimate ~14% DNA in Pf3. Such data provide constraints for structure models being developed for filamentous viruses.

The application of the turbidity method to filamentous viruses has involved measurements of scattering intensities that are reduced compared to spherical scatterers of the same mass and the use of somewhat complex scattering functions. We hope that these aspects of this particular study have not obscured the basic simplicity and convenience of making reliable, absolute turbidity measurements on solutions of macromolecules as they are being subjected to centrifugal fields.

References

Ansevin, A. T., Roark, D. E., & Yphantis, D. A. (1970) *Anal. Biochem. 34*, 237–261.

Babul, J., & Stellwagen, E. (1969) *Anal. Biochem. 28*, 216–221.

Beck, E., Sommer, R., Auerswald, E. A., Kurz, Ch., Zink, B., Osterburg, G., Schaller, H., Sugimoto, K., Sugisaki, H., Okamoto, T., & Takanami, M. (1978) *Nucleic Acids Res. 5*, 4495–4503.

Berkowitz, S. A. (1975) Ph.D. Thesis, New York University, New York.

Berkowitz, S. A., & Day, L. A. (1976) *J. Mol. Biol. 102*, 531–547.

Berkowitz, S. A., & Day, L. A. (1979) *Biophys. J. 25*, 280a.

Berne, B. J. (1974) *J. Mol. Biol. 89*, 755–758.

Bradley, D. E. (1974) *Biochem. Biophys. Res. Commun. 57*, 893–900.

Camerini-Otero, R. D., & Day, L. A. (1978) *Biopolymers 17*, 2241–2249.

Camerini-Otero, R. D., Franklin, R. M., & Day, L. A. (1974) *Biochemistry 13*, 3763–3773.

Carr, M. E., Jr., & Hermans, J. (1978) *Macromolecules 11*, 46–50.

Casassa, E. F., & Eisenberg, H. (1964) *Adv. Protein Chem. 19*, 287–395.

Cashin, W. M., & Debye, P. (1949) *Phys. Rev. 75*, 1307–1308.

Chen, F. C., Koopmans, G., Wiseman, R. L., Day, L. A., & Swinney, H. L. (1980) *Biochemistry 19*, 1373–1376.

Day, L. A., & Berkowitz, S. A. (1977) *J. Mol. Biol. 116*, 603–606.

Day, L. A., & Wiseman, R. L. (1978) in *The Single Stranded DNA Phages* (Denhardt, D. T., Dressler, D., & Ray, D. S., Eds.) pp 605–625, Cold Spring Harbor Laboratory, Cold Spring Harbor, NY.

Doty, P., & Steiner, R. (1950) *J. Chem. Phys. 18*, 1211–1220.

Eisenberg, H. (1971) *Proced. Nucleic Acid Res. 2*, 158.

Frangione, B., Nakashima, Y., Konigsberg, W., & Wiseman, R. L. (1978) *FEBS Lett. 96*, 381–384.

Frank, H., & Day, L. A. (1970) *Virology 42*, 144–154.

Gaskin, F., Cantor, C. R., & Shelanski, M. L. (1974) *J. Mol. Biol. 89*, 737–755.

Godfrey, J. E., & Eisenberg, H. (1976) *Biophys. Chem. 5*, 301–318.

Grumprecht, R. O., & Sliepcevich, C. M. (1953) *J. Phys. Chem. 57*, 90–95.

Heller, W., & Vassy, E. (1946) *J. Chem. Phys. 14*, 565.

Heller, W., & Tabibian, R. M. (1957) *J. Colloid Sci. 12*, 25–39.

Heller, W., Klevens, H. B., & Oppenheimer, H. (1946) *J. Chem. Phys. 14*, 566–567.

Horn, P. (1955) *Ann. Phys. (Paris) 10*, 386–434.

Horn, P., Benoit, H., & Oster, G. (1951) *J. Chim. Phys. Phys.-Chim. Biol. 48*, 530–535.

Josephs, R., & Harrington, W. F. (1967) *Proc. Natl. Acad. Sci. U.S.A. 58*, 1587–1594.

Kuo, T.-T., Huang, T.-C., Wu, R.-Y., & Yang, C.-M. (1967) *Bot. Bull. Acad. Sin. 8*, 246–254.

Ma, S. K., Schumaker, V. N., & Knobler, C. M. (1977) *J. Biol. Chem. 252*, 1728–1731.

Makowski, L., & Caspar, D. L. D. (1978) in *The Single Stranded DNA Phages* (Denhardt, D. T., Dressler, D., & Ray, D. S., Eds.) pp 626–643, Cold Spring Harbor Laboratory, Cold Spring Harbor, NY.

Marvin, D. A., & Hohn, B. (1969) *Bacteriol. Rev. 33*, 172–209.

Marvin, D. A., Wiseman, R. L., & Wachtel, E. J. (1974a) *J. Mol. Biol. 82*, 121–138.

Marvin, D. A., Pigram, W. J., Wiseman, R. L., Wachtel, E. J., & Marvin, F. J. (1974b) *J. Mol. Biol. 88*, 581–600.

Newman, J., & Carlson, F. D. (1980) *Biophys. J. 29*, 37–48.
Newman, J., Swinney, H. L., & Day, L. A. (1977) *J. Mol. Biol. 116*, 593–606.
Sanger, F., Coulson, A. R., Friedman, T., Air, G. M., Barrell, B. G., Brown, N. L., Fiddes, J. C., Hutchinson, C. A., III, Slocumbe, P. M., & Smith, M. (1978) *J. Mol. Biol. 125*, 225–246.
Stanisich, V. A. (1974) *J. Gen. Microbiol. 84*, 332–342.
Studier, F. W. (1965) *J. Mol. Biol. 11*, 373–390.
Tabor, B. E. (1972) in *Light Scattering from Polymer Solutions* (Huglin, M. B., Ed.) p 1, Academic Press, New York.
Timasheff, S. N., & Townsend, R. (1970) in *Physical Principles and Techniques of Protein Chemistry* (Leach, S. J., Ed.) Part B, p 187, Academic Press, New York.
Wall, J. (1971) Ph.D. Thesis, University of Chicago, Chicago, IL.
Wiseman, R. L., & Day, L. A. (1977) *J. Mol. Biol. 116*, 607–611.
Yamamoto, K. R., Alberts, B. M., Benzinger, R., Lawhorne, L., & Treiber, G. (1970) *Virology 40*, 734–744.

Molecular Cloning of Seven Mouse Immunoglobulin κ Chain Messenger Ribonucleic Acids†

Nicholas M. Gough, Elizabeth A. Webb, Suzanne Cory, and Jerry M. Adams*

ABSTRACT: To provide access to multiple immunoglobulin κ chain variable region sequences, we have constructed plasmid clones bearing duplex DNA sequences complementary to κ mRNAs isolated from seven different mouse plasmacytomas (McPC 603, MOPC 41A, MOPC 173, MOPC 21, BFPC 61, HPC 76, and S107). Duplex complementary DNA (cDNA) was synthesized by using reverse transcriptase and DNA polymerase I, and the longest cDNA molecules, selected by gel filtration, were inserted into the *Pst*I site of the vector pBR322 by the dG·dC tailing procedure, which permits subsequent excision of the cDNA insert [Bolivar, F., Rodriguez, R. L., Greene, P. J., Betlach, M. C., Heyneker, H. L., & Boyer, H. W. (1977) *Gene 2*, 95]. The oligo(dG·dC) tails, sized by depurination of insert sequences labeled at 3′ termini, were between 11 and 23 nucleotides long. Clones bearing κ sequences were identified by in situ colony hybridization using [^{32}P]cDNA made on a substantially purified κ mRNA as a probe. Identity was confirmed in several ways, including the ability of a cloned cDNA sequence to specifically arrest translation of κ mRNA and the precise correlation of restriction endonuclease cleavage maps with known amino acid sequences. Clones derived from each of the seven mRNAs have insert sequences 915–1000 base pairs long, which represent nearly the full length of the κ mRNA. Detailed restriction maps confirm that the clones bear seven distinct V_κ sequences, as well as C_κ and 3′ noncoding regions. The maps of the C region halves of all clones are identical, providing evidence for a unique C_κ sequence. The maps of two clones confirm that there is a 5′ noncoding region in κ mRNAs and indicate that it is between 68 and 210 nucleotides in length. Restriction mapping has also revealed an apparent cloning aberration, the presence of an *Mbo*II site toward the 3′ terminus of one of the cDNA sequences, at a position where there is no *Mbo*II site in the mRNA sequence.

Immunoglobulins are composed of light and heavy chains, each having an N-terminal variable (V)[1] region and a C-terminal constant (C) region (Hilschmann & Craig, 1965; for a review, see Gally, 1973). A key molecular problem presented by the immunoglobulin (Ig) gene system is how V region diversity is acquired—through evolutionary or somatic processes, or both (Weigert et al., 1970; Hood et al., 1975). κ chains, the predominant class of light chains in the mouse, exhibit extensive variability, although V_κ regions can be divided into "subgroups" or "isotypes" which have very similar N-terminal amino acid sequences (Potter, 1977). Each subgroup presumably is encoded in the germ line, but it remains uncertain whether each member of such a group is inherited. Evidence that the germ line contains multiple related V_κ genes has come recently from molecular cloning (Seidman et al., 1978a), but somatic processes have also been implicated by evidence from saturation hybridization that there are not enough related V_κ genes to account for the diversity within an isotype (Valbuena et al., 1978).

A deeper analysis of κ chain diversity requires access to a variety of V_κ nucleotide sequences representing different isotypes. The difficulty of isolating κ mRNAs in sufficient purity and quantity can be surmounted by recombinant DNA techniques. In particular, chimeric plasmids containing DNA sequences complementary to individual mRNAs allow production of large quantities of pure structural gene sequences, thus greatly facilitating hybridization and sequence studies (Rougeon et al., 1975; Higuchi et al., 1976; Maniatis et al., 1976; Rabbitts, 1976; Rougeon & Mach, 1976). Plasmids carrying sequences complementary to five κ mRNAs have recently been reported (Mach et al., 1977; Lenhard-Schuller et al., 1978; Schibler et al., 1978; Seidman et al., 1978b; Strathearn et al., 1978; Wall et al., 1978).

In order to generate an expanded set of pure κ nucleotide sequences, we have cloned κ mRNAs from seven different mouse plasmacytomas, representative of different V_κ isotypes. To ensure that V region sequences were represented, we prepared duplex cDNA under conditions that favor longer transcripts (Efstratiadis et al., 1976; Kacian & Myers, 1976)

† From the Molecular Biology Laboratory, The Walter and Eliza Hall Institute of Medical Research, Melbourne, Victoria 3050, Australia. *Received September 24, 1979.* This work was supported by the U.S. National Cancer Institute (RO1 CA 12421), The American Heart Association, and the National Health and Medical Research Council (Canberra).

[1] Ig, immunoglobulin; C, constant region; V, variable region; cDNA, complementary DNA; poly(A), poly(adenylic acid); EDTA, ethylenediaminetetraacetic acid; bp, base pair(s); $NaDodSO_4$, sodium dodecyl sulfate; Hepes, *N*-2-hydroxyethylpiperazine-*N*′-2-ethanesulfonic acid.

0006-2960/80/0419-2702$01.00/0